

# Identification of the under-tie pad material characteristics for stress state reduction

Proc IMechE Part F:  
*J Rail and Rapid Transit*  
0(0) 1–11  
© IMechE 2019  
Article reuse guidelines:  
sagepub.com/journals-permissions  
DOI: 10.1177/0954409719890156  
journals.sagepub.com/home/pif



Jacob M Branson<sup>1,2</sup> , Marcus S Dersch<sup>2</sup>,  
Arthur de Oliveira Lima<sup>2</sup> , J Riley Edwards<sup>2</sup> and  
Josue Cesar Bastos<sup>2</sup>

## Abstract

The degradation of ballast particles and concrete crossties in heavy-haul railroad tracks poses problems such as inhibiting proper drainage and disturbing track geometry. Under-tie pads offer a solution to reduce crosstie–ballast stresses by improving load distribution through the track structure and reducing pressures on ballast particles and the crosstie surface. Despite the emergence of under-tie pads on heavy-haul corridors, optimal characteristics for the reduction of the tie–ballast stress state have not been defined in literature. In this research, several under-tie pad products and generic materials with various thicknesses and hardnesses were studied to identify appropriate properties of under-tie pad products for pressure distribution. The findings from this research provide an insight into how material characteristics influence the pressure mitigation performance of under-tie pads. Results from this study indicate that thickness is the most crucial metric determining under-tie pad performance in reducing ballast degradation; hardness and material type also have an effect, but to a lesser degree.

## Keywords

under-tie pads, matrix-based tactile surface sensors, railroad track infrastructure, pressure distribution, materials optimization, crosstie

Date received: 8 April 2019; accepted: 19 October 2019

## Introduction

Ballast serves as an essential component to conventional railroad track by supporting loads, providing track stability, and permitting drainage.<sup>1</sup> Preserving ballast on rail corridors is of crucial importance to railroad companies, as capital expenditures related to ballast maintenance and renewal typically account for around 11% of track expenses on the railroad network of the United States.<sup>2</sup> This maintenance is required given that there is degradation and wear of ballast that compromises its ability to maintain track alignment over time and consequently jeopardizes safety.<sup>3</sup> Degraded ballast also leads to fouling, a condition that accelerates track settlement, prevents effective surfacing, and impedes drainage.<sup>1,4</sup> Therefore, preventing ballast degradation is crucial to maintaining proper track infrastructure.

One emerging solution to increase ballast service life and preserve track geometry is the installation of resilient materials within the track substructure.<sup>5</sup> One such product is an under-tie pad (UTP), an elastic pad that is inserted onto the bottom of a crosstie. UTPs

are commonly produced from rubber, polyurethane, or EVA products, though other polymeric materials can be used.<sup>6</sup> Other materials including bonded recycled rubber chips and used automobile tires have also been studied for potential usage.<sup>7</sup> UTPs are often bonded directly to the bottom surface of a concrete crosstie during production, though they can also be added to various crosstie types post manufacturing using adhesives or staples. UTPs serve two major purposes: mitigating noise and vibrations from train passes and reducing stresses at the interface

<sup>1</sup>Rail Transportation and Engineering Center – RailTEC, CEE University of Illinois at Urbana-Champaign, Urbana, IL, USA

<sup>2</sup>Department of Civil and Environmental Engineering – CEE University of Illinois at Urbana-Champaign – Civil Engineering Laboratory, Urbana, IL, USA

### Corresponding author:

Jacob M Branson, University of Illinois at Urbana-Champaign, 205 N Mathews Ave, B-118, Newmark Engineering Lab, MC-250, Urbana, IL 61801, USA.

Email: jbranso2@illinois.edu

between the bottom of a crosstie and ballast beneath it.<sup>8–10</sup> With regard to the latter, UTPs can be used to reduce substructure stiffness at locations such as ballasted bridge decks and special trackwork to minimize high-impact forces associated with track transitions.<sup>11</sup> Prior research has shown that the addition of UTPs engages more ties to more evenly distribute loads along the track structure.<sup>12</sup> Consequently, the time between surfacing cycles can be increased as track geometry is maintained over longer time periods.<sup>13,14</sup>

In addition, UTPs can effectively minimize contact pressures between individual ballast particles and the crosstie bottom. As load is applied to a crosstie and consequently to a UTP, the component will conform to the particles of ballast it contacts and will increase the contact surface area between it and the ballast. Prior research has shown an increase in contact between a crosstie and ballast from 1 to 9% without UTPs<sup>15</sup> to as high as 35% with UTPs.<sup>16</sup> By engaging more contact between the crosstie and ballast particles, both components experience lower overall stresses. At the same time, the UTP protects each surface from direct wear from abrasion.<sup>9</sup> Ultimately, UTPs enable the potential to reduce damage on both the crosstie bottom and ballast particles and increase the life cycles of each component.

Stress optimization is not the only metric that should be considered when selecting a UTP product. Components used in heavy-haul applications are exposed to high loads as well as changes in moisture and temperature, factors that should also be considered in UTP performance.<sup>17,18</sup> Further, some UTP products have raised concerns of reduced track stability by causing ballast particles to migrate over time, particularly in curves.<sup>19</sup> Thus, a UTP's effects on ballast migration must also be considered. The primary objective of this paper, however, is to study the material properties of potential UTP materials for their effectiveness at reducing ballast degradation in a manner that is realistic for UTP product development. General thresholds for ballast degradation and concrete abrasion are provided as a means of comparison for each material. While fatigue performance and effects on ballast movement are areas of interest for UTP products, they fall outside the scope of this paper.

Three prevalent material characteristics—material type, thickness, and hardness—were analyzed to determine their performance at reducing contact pressures. To understand how these characteristics affect UTP performance, an array of generic material samples was compiled for this study. Two common polymeric materials, neoprene and polyurethane, in a variety of thickness and hardness measurements were subjected to laboratory experimentation to analyze how each mitigates contact pressures at the ballast–tie interface under static conditions. While some of characteristics, such as thickness, have been studied individually through prior research, this paper aims to

discuss all three characteristics coincidentally.<sup>20</sup> It is important to note that neoprene and polyurethane have broad product scopes that were not all included in this research. Polyurethane, for example, comes in many basic forms fit for various applications, which must be considered when drawing conclusions from this study.<sup>21</sup> Additionally, three UTP products were studied and compared with the generic materials. The results presented within this paper provide information about how UTP material properties affect the ballast–tie stress state.

## Materials and methods

### Materials

Samples were selected to form a representative sampling of both actual and possible UTP products. Two closed-cell polymeric generic material samples were selected for analysis in this study: neoprene and polyurethane. These materials were chosen owing to their likelihood of use in UTP products. The material types were acquired from a materials distributor with hardness values between 40A and 70A on the Shore A scale. Furthermore, four different material thicknesses—0.4 mm (1/64"), 3.2 mm (1/8"), 6.4 mm (1/4"), and 9.5 mm (3/8")—were selected to investigate how thickness influences UTP performance. Figure 1 shows a portion of the generic material samples analyzed in this study. Samples with both a thickness of 0.4 mm (1/64") and a hardness of 40A were unavailable and therefore not included in this study. In addition to the generic material samples, three types of commercially available UTP products were studied in this research and labelled A–C. All three were constructed from polyurethane with manufacturer-provided static bedding modulus values ( $C_{stsat}$ ) between 0.10 and 0.15 N/mm<sup>3</sup>. Samples A and B contained a fibrous layer designed to protect the polyurethane from damage and distribute loads into the ballast, but sample C was not so equipped.

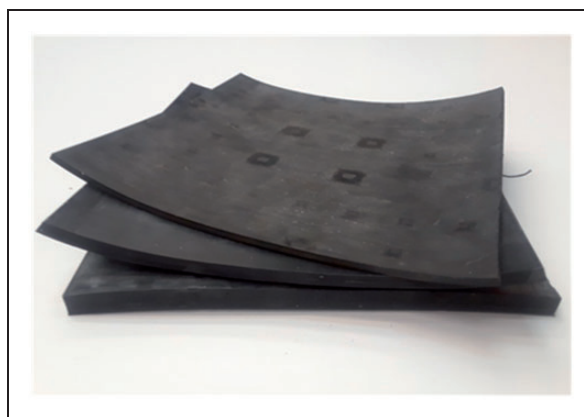


**Figure 1.** Neoprene 40A samples in 3.2 mm (1/8") (top), 6.4 mm (1/4"), and 9.5 mm (3/8") thicknesses.

For experimentation, each generic material sample was cut into  $20.3 \times 20.3$  cm ( $8 \times 8$  in.) square specimens and each UTP product was cut into  $21.6 \times 21.6$  cm ( $8.5 \times 8.5$  in.) squares. Thickness readings were taken at eight points on each specimen using a micrometer. The mean thickness values for each specimen were then compiled to serve as composite values. Descriptions of each material used in this study, along with their mean sample thicknesses, are given in Table 1.

### Experimentation methods

Experimentation on the selected material samples followed a modified procedure from the 2017 European

**Table 1.** Description of the generic materials and UTP products.

Sample	Material	Nominal thickness (in.)	Hardness	Actual thickness mm (in.)
1	Neoprene	1/8	40A	3.18 (0.125)
2	Neoprene	1/8	60A	3.28 (0.129)
3	Neoprene	1/8	70A	3.43 (0.135)
4	Neoprene	1/4	40A	6.40 (0.252)
5	Neoprene	1/4	60A	6.07 (0.239)
6	Neoprene	1/4	70A	6.40 (0.252)
7	Neoprene	3/8	40A	9.19 (0.362)
8	Neoprene	3/8	60A	9.53 (0.375)
9	Neoprene	3/8	70A	9.70 (0.382)
10	Polyurethane	1/8	40A	3.25 (0.128)
11	Polyurethane	1/8	60A	3.12 (0.123)
12	Polyurethane	1/4	40A	6.22 (0.245)
13	Polyurethane	1/4	60A	6.38 (0.251)
14	Polyurethane	3/8	40A	9.25 (0.364)
15	Polyurethane	3/8	60A	9.19 (0.362)
16	Neoprene	1/64	60A	0.41 (0.016)
17	Neoprene	1/64	70A	0.41 (0.016)
UTP A	Polyurethane	—	63A	10.31 (0.406)
UTP B	Polyurethane	—	48A	10.82 (0.426)
UTP C	Polyurethane	—	70A	10.64 (0.419)

Note: Each sample consisted of three replicates.

UTP: under-tie pad.

Standard (EN 16730), hereafter referred to as the EN.<sup>22</sup> The EN's standard test for the determination of static bedding modulus was utilized for this study, as diagramed in Figure 2. This test procedure is comprised of four preconditioning cycles of loading followed by a fifth cycle for data collection. To account for higher axle loads found on North American railroads, the EN's recommended load levels were increased to be representative of the 95th percentile nominal heavy axle load of 356 kN (80 kips) as outlined in AREMA.<sup>18,23</sup> Three key outcomes—maximum pressure, average pressure of the loaded area, and contact area—were evaluated as a part of this study. Conforming to the EN, an engineered geometric ballast plate (GBP) was used to simulate the support condition characteristics of ballast as shown in Figure 3. The GBP is made of steel and consists of symmetrically arranged nodes designed to replicate the contact of ballast particles. Prior research has shown that the support from the GBP results in lower pressure characteristics than actual ballast support, but its ease of implementation and repeatability

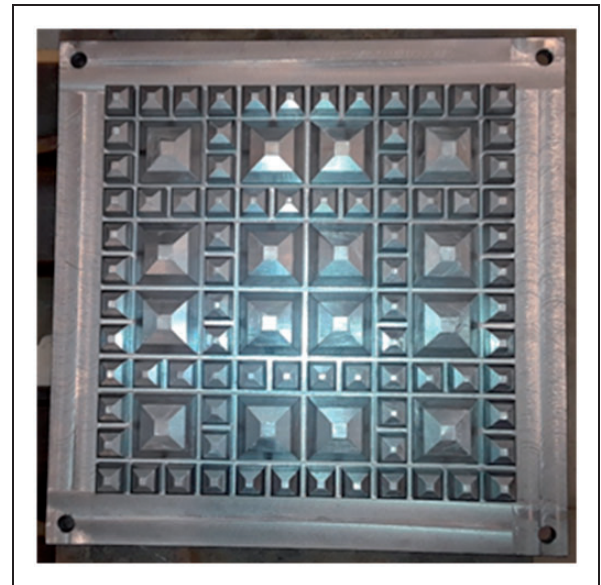


**Figure 3.** GBP based on EN 16730:2016 used for the support condition to represent ballast particles and reduce variability between replicates.

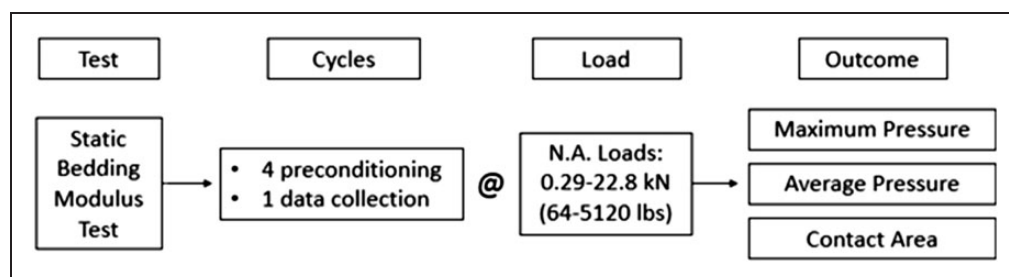


**Figure 2.** Test procedure based on EN 16730:2016 used for this study.

among replicates made it preferable for use in this study.<sup>24</sup> For experiments conducted during this study, the GBP served as the bottom support condition.

Matrix-based tactile surface sensors (MBTSS) were used to measure the contact pressures acting on each sample under static loading. MBTSS consist of rows and columns of semi-conductive material arranged in a grid between two layers of film. When the sensor is subjected to contact between two objects, the semi-conductive material experiences a change in resistivity that is measured through a data-acquisition handle and transmitted to a computer. Data are measured by individual pressure-sensing locations, called sensels, that are formed between the intersecting rows and columns of the semi-conductive material. The MBTSS used for this experimentation consist of 1936 total sensels, each with an area of  $0.31 \text{ cm}^2$  ( $0.0484 \text{ in.}^2$ ).<sup>25</sup> Data from the MBTSS are output as a number corresponding to force acting on each sensel that can be calibrated based on the applied loads. The matrix design of MBTSS allows for both qualitative and quantitative analysis of pressure distribution. Contact area can also be determined through the sum of the area of all loaded sensels during each test. Polytetrafluoroethylene (PTFE) and biaxially-oriented polyethylene terephthalate (BoPET) were used to protect the MBTSS during loading as described in prior applications.<sup>25–27</sup> The total thickness of the MBTSS and protection layers was  $0.76 \text{ mm}$  ( $0.03 \text{ in.}$ ). While thin rubber has also been used as MBTSS protection,<sup>16,28</sup> it was ruled out as a potential protective material due to its qualities of pressure distributions and the subsequent effects on the results of the materials that were the focus of the experimentation. A picture of an MBTSS and a diagram of the protective layering is provided in Figure 4.

MBTSS have been used in prior railway research to quantify pressures at both the tie plate/crosstie interface,<sup>25,29</sup> the timber crosstie/ballast interface,<sup>28,30</sup> and

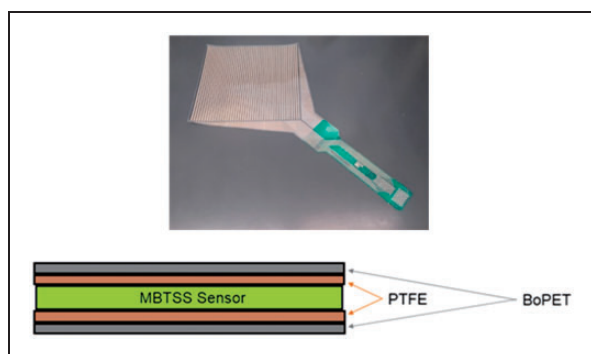


**Figure 4.** Picture of MBTSS used in this study and diagram of protective layering.

MBTSS: matrix-based tactile surface sensors; PTFE: polytetrafluoroethylene; BoPET: biaxially-oriented polyethylene terephthalate.

the concrete crosstie/ballast interface.<sup>16</sup> They have also been utilized to study the effects of pressure on rail seat deterioration.<sup>25,27,31</sup> Additionally, UTP contact areas have been measured using other sensing technologies, including pressure paper.<sup>32</sup>

Experimentation was conducted using a vertically-mounted hydraulic actuator that applied predetermined loads onto each specimen, which were placed directly on the GBP. An MBTSS was then inserted above the specimen and the system was loaded. This arrangement was selected over inserting the MBTSS between the UTP specimen and the GBP to avoid the MBTSS sensor ‘bridging’ the gaps between nodes on the GBP. A diagram of the experimental setup is provided in Figure 5.

## Results and discussion

To serve as benchmarks for the performance of each sample and the impacts of each material characteristic, the authors established key stress thresholds for ballast and concrete crosstie degradation based on prior research. Studies on ballast particle crushing indicate that the force threshold for ballast particle breakage is upwards of  $11 \text{ MPa}$  ( $1600 \text{ psi}$ ) depending on particle size and characteristics.<sup>33,34</sup> Other research has concluded that the fatigue strength of concrete is approximately 50% of its ultimate compressive strength.<sup>35,36</sup> Therefore, a threshold for concrete fatigue crushing under repeated loading was established at  $24.1 \text{ MPa}$  ( $3500 \text{ psi}$ ), assuming a concrete mix with an ultimate compressive strength of  $48.2 \text{ MPa}$  ( $7000 \text{ psi}$ ) as recommended for concrete crossties by AREMA.<sup>23</sup>

The results will allow for analysis of each characteristic to determine which are relevant to the design or selection of a UTP product for optimal pressure mitigation performance. It must be noted that knowing one predictor characteristic alone is not necessarily adequate to predict the full performance of the UTP. However, the focus of this study is to analyze each characteristic independently to determine the degree at which each impacts pressure performance.

An analysis of variance (ANOVA) was performed on the maximum pressure results to determine the statistical significance of each variable studied in this research. All samples were included in the ANOVA

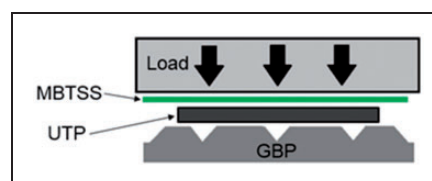


**Figure 5.** Diagram of the experimental setup for quantifying pressure under UTP materials.

MBTSS: matrix-based tactile surface sensors; GBP: geometric ballast plate; UTP: under-tie pad.



except the 0.4 mm (1/64") samples, a thickness considered not realistic for UTP usage. The ANOVA was carried out with a significance factor  $\alpha = 0.05$  and assumptions of constant variance and normality of residuals were adequately met. Variables A, B, and C are binary indicators of material type classification in the statistical analysis. As indicated from the ANOVA results provided in Table 2, thickness is the most statistically significant variable in terms of pressure mitigation performance of UTPs. Therefore, while hardness plays a minor role, thickness appears to be the main characteristic affecting the mitigation of pressures. Furthermore, the material types studied

in this research did not exhibit statistically significant differences in pressure mitigation performance.

A plot of maximum pressures is presented in Figure 6 with data points representing the mean maximum pressure value from three replicates of the same sample type. The results from this figure reinforce the findings of the ANOVA, particularly that thickness appears to be the most impactful characteristic for pressure reduction. Notably, the pressures of all 3.2 mm (1/8"), 6.4 mm (1/4"), and 9.5 mm (3/8") specimens, regardless of material type and hardness, fall well below the thresholds for both ballast particle crushing and concrete fatigue crushing. In addition, a general correlation between harder materials and increased maximum pressures can be distinguished. Maximum pressures rise above the threshold for ballast particle crushing for both hardness samples of 0.4 mm (1/64") neoprene. Furthermore, the 60A specimens of 0.4 mm (1/64") neoprene also reached the threshold of concrete fatigue crushing. All three UTP product types resulted in maximum pressures that were approximately 5–10 times below the threshold for ballast particle crushing. Therefore, it appears that the UTP products studied are thicker than required to obtain adequate pressure mitigation performance.

**Table 2.** ANOVA table results (a) and parametric significance (b).

(a)

	DF	Sum of squares	Mean square	F value	Pr > F
Model	6	3,024,125	504,021	98.68	<.0001
Error	47	240,068	5108		
Calculated total	53	3,264,193			

(b)

Variable	t value	Type III sum of squares	P
Intercept	9.27	439,387	<.0001
Neoprene	2.09	22,376	0.0418
A	1.55	12,240	0.1283
B	2.81	40,200	0.0073
C	-1.17	7052	0.2459
Hardness	6.35	205814	<.0001
Thickness	-20.05	2053761	<.0001

### Effect of thickness

Figure 7 provides both a quantitative and qualitative comparison between various thicknesses with 60A neoprene samples serving as the representative case for comparison. A general correlation between pressure distribution and specimen thickness is evident given lower pressures and increased surface areas are observed as thickness increases. The 0.4 mm (1/64") specimens do not have adequate material to distribute the loads being applied and pressures are

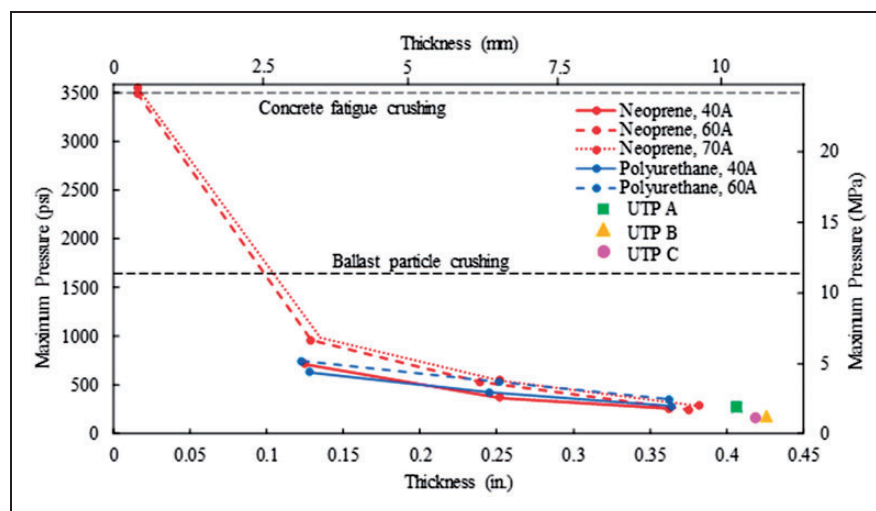


**Figure 6.** Maximum pressure by material, thickness, and hardness with relevant thresholds. UTP: under-tie pad.

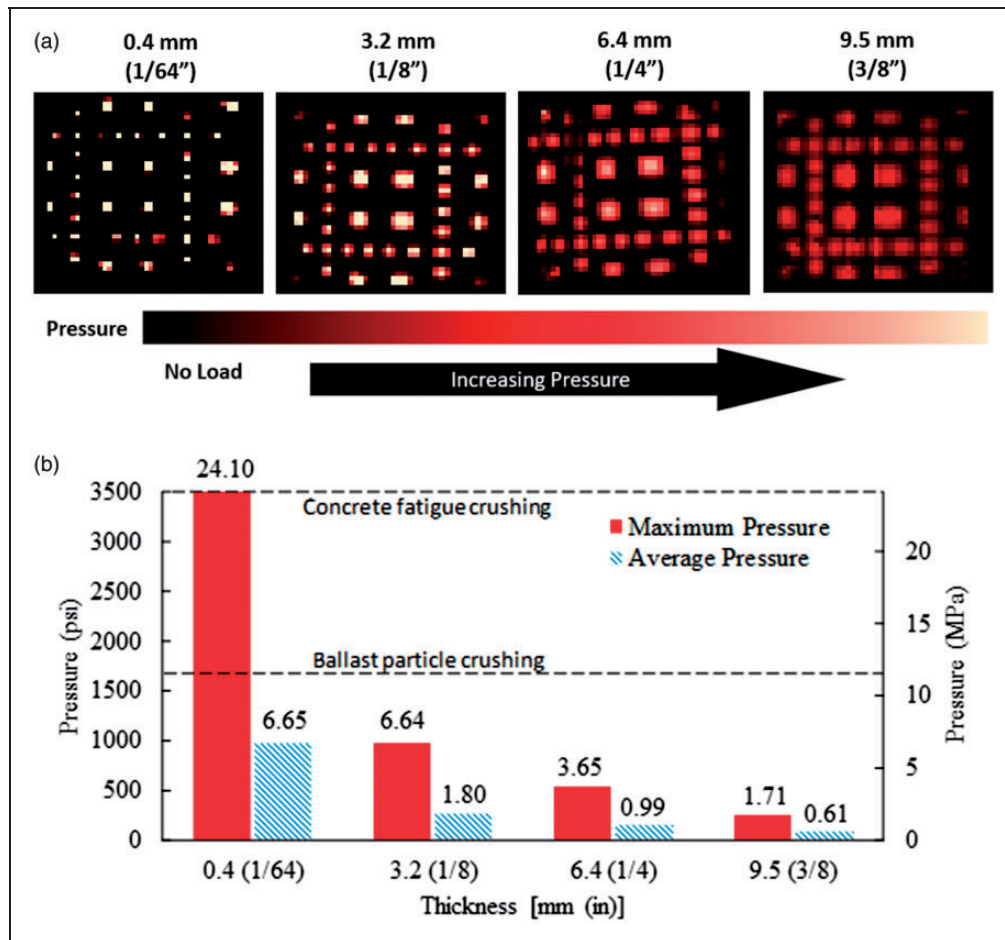


**Figure 7.** (a) Pressure distribution of 60A neoprene specimens at various thickness values; (b) maximum and average pressures for specimens of varying thicknesses.

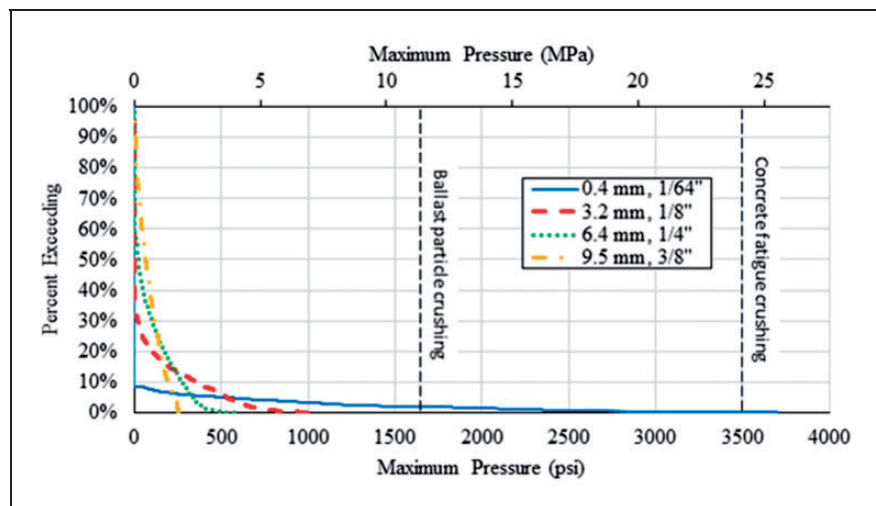


**Figure 8.** Percent exceedance of specimen area for 60A neoprene specimens at various thicknesses.

therefore concentrated highly around the GBP nodes. Thicker samples—the 9.5 mm (3/8") sample in particular—provide a greater reduction in both maximum and average pressure as they conform more to the objects they are in contact with, as expected.

Figure 8 shows the distribution by thickness of sensor pressures during experimentation of the 60A neoprene specimens when subjected to maximum loading. This figure contains data from all sensors from all three replicates of each noted sample type.

The maximum recorded pressure was just under 25.5 MPa (3700 psi) from the 0.4 mm (1/64") thick specimens, with only 8.5% of the total area experiencing any contact. The curves for the other three samples tend to become more uniform as thickness increases. This is indicative of more even load distribution through increased contact area and a subsequent reduction in maximum pressure from samples with greater thickness.

### Effect of hardness

Figure 9 shows the comparison of the pressure distribution at various hardness values with 3.2 mm (1/8") neoprene serving as the representative case for comparison. In each case, high pressure areas are located at the center of the larger nodes on the GBP. However, the images of the 60A and 70A hardness specimens show larger densities of high pressures at each node, indicating that the softer specimen is more effective at spreading loads over an increased surface area and subsequently reducing the average pressure of the system. This outcome was expected prior to running the experiment. The quantitative data presented in Figure 9(b) indicate that none of the

hardness values exceeded the thresholds for ballast particle or concrete fatigue crushing.

### Effect of material type

Figure 10 shows the comparison of pressure distribution characteristics between typical neoprene and polyurethane specimens, each at 3.2 mm (1/8") thickness and 40A hardness. Similar distribution patterns are visible between the neoprene and polyurethane specimens with areas of high pressure concentrated at each of the larger nodes on the GBP. Qualitatively, the areas of pressure against each node are comparable for each type of material in this specific case. The graph in Figure 10(b) shows that the materials yield similar pressure magnitudes that fall below the key thresholds.

### Performance of UTP products

Due to the variability in polyurethane products, direct comparisons between the UTP products and the generic polyurethane materials were difficult. However, since the three UTPs were of similar thicknesses, the results from each UTP product allowed for

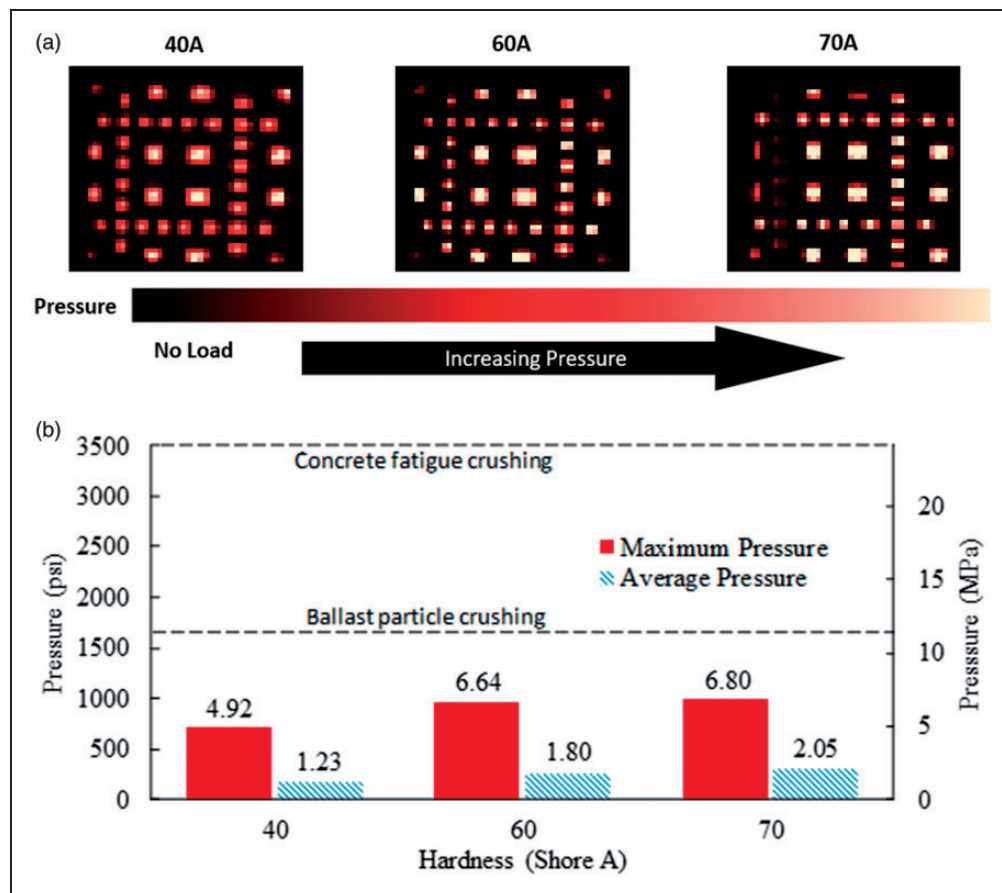


**Figure 9.** (a) Pressure distribution of 3.2 mm (1/8") neoprene specimens at 40A, 60A, and 70A hardness; (b) maximum and average pressure results from specimens of various hardness values.

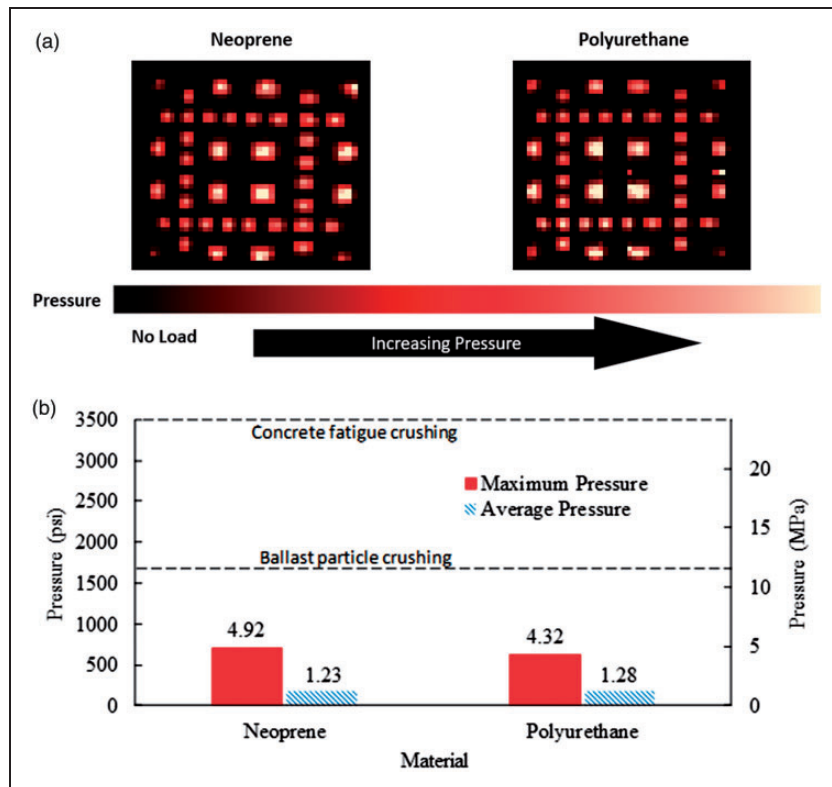


**Figure 10.** (a) Maximum and average pressure results from neoprene and polyurethane specimens; (b) Pressure distribution of neoprene and polyurethane samples with 3.2 mm (1/8") thickness and 40A hardness.

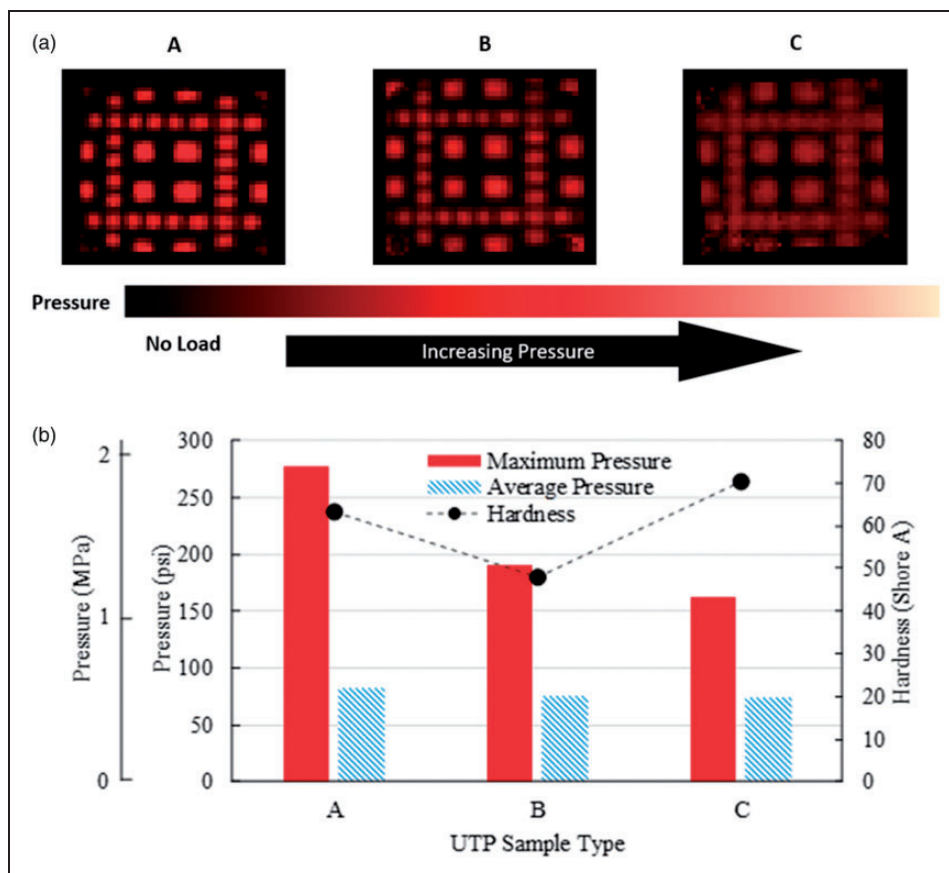


**Figure 11.** (a) Pressure distribution of UTP samples; (b) maximum and average pressures of each UTP sample, along with material hardness.



comparisons between hardness and sample type. While each UTP product was approximately 10 mm (0.04 in.) thick, each product was manufactured differently. Sample A consisted of finely grained polyurethane with a protective fiber layer approximately 3 mm (0.12 in.) thick. Sample B consisted of the same protective fiber layer over polyurethane with thicker grains that tore when cut with a utility knife. Both samples were advertised for use in protecting ballast and absorbing ground-borne vibrations. Sample C was marketed only as a heavy-haul product (no vibration absorption) and consisted of firm polyurethane with a hardened ‘crust’ on one side that was too thin to be measured. While the exact properties of the polyurethane materials were unable to be discerned from the samples, the visual characteristics and varying hardness values of each sample indicate that different base materials were used in each UTP product.

Figure 11 shows the visual and quantitative results from the UTP product pressures experiments and has been scaled down from previous plots to analyze trends in greater resolution. Since the thickness for each UTP is approximately equal, the results from each sample allow for further comparison between the effects of hardness and material type. The plot of maximum and average pressure along with material hardness in Figure 11(b) shows no correlation between hardness and pressure for the UTP products. UTPs A and B show an expected trend between lower hardness and lower pressures. However, UTP C, the hardest of the UTP samples, yields the lowest maximum pressures of any of the materials in this study. Since each sample type consists of a different material of a similar thickness, it appears that material type has a slight influence on the pressure distribution characteristics of UTP components. While this contrasts with the findings from the generic materials discussed above, it is apparent that material type, along with other potential factors including protective layering, can impact a UTP’s pressure mitigation performance.

## Conclusions

Results from this research suggest that thickness is the most critical characteristic to consider when selecting a product for pressure mitigation. Hardness and material type both showed evidence of effecting pressure mitigation performance of UTPs but to a smaller extent than thickness. It is important to consider that the authors only studied materials, thicknesses, and hardnesses that were plausible for UTP designs. The main findings from this research include:

1. All samples thicker than 3.2 mm (1/8") yielded maximum pressures below the thresholds for both ballast particle crushing and concrete fatigue crushing. For 0.4 mm (1/64") samples, maximum

pressures increased to levels that exceeded the threshold for ballast crushing for both 40A and 60A hardness values.

2. It appears that the UTP products can be further optimized in terms of thickness to offer adequate pressure reduction performance with less material.
3. Comparison of the generic materials indicates that a general trend exists between softer materials and greater pressure reduction. Statistical analysis reveals that hardness does significantly affect pressure results, though to a lesser degree than thickness.
4. The two types of generic materials studied—neoprene and polyurethane—yielded similar trends in pressure distribution which were reinforced through statistical analysis. However, the UTP products, which were constructed out of different polyurethane materials, showed differences in pressure distribution behavior.

Further experimentation is needed to ensure adequate resistance of these materials to fatigue. Since each specimen in this study was only subjected to five cycles of loading, it is unknown how each material sample will perform over the duration of its life cycle or how it will perform under varying temperature and moisture conditions. Investigating the effects of freeze/thaw and fatigue loading is crucial to understanding how UTPs will fare over time in the harsh environment that they are in. In addition, the effects of the studied materials on ballast migration were not considered during this study. Consequently, future studies of UTP optimization should consider these effects.

## Acknowledgements

The contents of this report reflect the views of the authors, who are responsible for the facts and the accuracy of the information presented herein. This document is disseminated under the sponsorship of the U.S. Department of Transportation’s University Transportation Centers Program, in the interest of information exchange. The U.S. Government assumes no liability for the contents or use thereof. Laboratory experimentation for this paper was performed at the Research and Innovation Laboratory (RAIL) at the Harry Schnabel, Jr. Geotechnical Laboratory in Champaign, IL. The loading frame utilized for this experimentation was owned by Progress Rail Services (PRS).

## Declaration of Conflicting Interests


The author(s) declared no potential conflicts of interest with respect to the research, authorship, and/or publication of this article.


## Funding

The author(s) disclosed receipt of the following financial support for the research, authorship, and/or publication of this article: This research has been primarily supported through funding from the National University Rail Center

(NURail), a US DOT OST-R Tier 1 University Transportation Center. Jacob Branson has been funded in part through a grant from PRS. Riley Edwards has been funded in part through grants to the UIUC Rail Transportation and Engineering Center (RailTEC) from CN and Hanson Professional Services.

### ORCID iDs

Jacob M Branson  <https://orcid.org/0000-0002-8289-7581>

Arthur de Oliveira Lima  <https://orcid.org/0000-0002-9642-2931>

J Riley Edwards  <https://orcid.org/0000-0001-7112-0956>

### References

1. Selig ET and Waters JM. *Track geotechnology and sub-structure management*. London: Thomas Telford, 1994.
2. Association of American Railroads. *Total annual spending: 2015 data*. Washington: Author, 2015, p.8.
3. Huang H, Tutumluer E and Dombrow W. Laboratory characterization of fouled railroad ballast behavior. *Transp Res Rec* 2009; 2117: 93–101.
4. Tutumluer E, Huang H, Hashash YMA, et al. Gradations affecting ballast performance using discrete element modeling (DEM) approach. In: *Proceedings of the American railway engineering and maintenance of way association conference*, Chicago, IL, 20–23 September 2009.
5. Navaratnarajah SK and Indraratna B. Use of rubber mats to improve the deformation and degradation behavior of rail ballast under cyclic loading. *J Geotech Geoenviron Eng* 2017; 143.
6. Witt S. *The influence of under sleeper pads on railway track dynamics*. MSc Thesis, Linköping University Institute of Technology, Linköping, SV, 2008.
7. Sol-Sánchez M, Moreno-Navarro F and Rubio-Gámez MC. The use of deconstructed tires as elastic elements in railway tracks. *Constr Build Mater* 2014; 7: 5903–5919.
8. Nimbalkar S, Indraratna B, Dash SK, et al. improved performance of railway ballast under impact loads using shock mats. *J Geotech Geoenviron Eng* 2012; 138: 281–294.
9. Indraratna B, Nimbalkar S, Navaratnarajah SK, et al. Use of shock mats for mitigating degradation of railroad ballast. *Sri Lankan Geotech J – Special Issue on Ground Improvement* 2014; 6: 32–41.
10. Navaratnarajah SK, Indraratna B and Ngo NT. Influence of under sleeper pads on ballast behavior under cyclic loading: experimental and numerical studies. *J Geotech Geoenviron Eng* 2018; 144.
11. Li D and Davis D. Transition of railroad bridge approaches. *J Geotech and Geoenviron Eng* 2005; 131: 1392–1398.
12. Johansson A, Nielsen JCO, Bolmsvik R, et al. Under sleeper pads – Influence on dynamic train-track interaction. *Wear* 2008; 265: 1479–1487.
13. Schneider P, Bolmsvik R and Nielsen JCO. In situ performance of a ballasted railway track with under sleeper pads. *J Rail Rapid Transit* 2010; 225(Part F): 299–309.
14. Li D, Otter D and Carr G. Railway bridge approaches under heavy axle load traffic: problems, causes, and remedies. *J Rail Rapid Transit* 2010; 224(Part F): 383–390.
15. Lichtberger B. *Track compendium: formation, permanent way, maintenance, economics*. Hamburg: Eurailpress, 2005.
16. Grabe PJ, Mtshotana BF, Sebati MM, et al. The effects of under-sleeper pads on sleeper-ballast interaction. *J South Afr Inst Civil Eng* 2016; 58: 35–41.
17. Van Dyk BJ, Edwards JR, Dersch MS, et al. Evaluation of dynamic and impact wheel load factors and their application in design processes. *J Rail Rapid Transit* 2016; 231: 33–43.
18. Lima, A de O, Dersch MS, Qian Y, et al. Laboratory mechanical fatigue performance of under-ballast mats subjected to North American loading conditions. In: *Proceedings of 11th international heavy haul association conference*, Cape Town, ZA, 2–6 September 2017.
19. McHenry MT. Engineered pads for railroad track improvement. In: *23rd annual AAR research review*, Colorado Springs, CO, 27–28 March 2018.
20. Sol-Sánchez M, Moreno-Navarro F and Rubio-Gámez MC. The use of deconstructed tire rail pads in railroad tracks: impact of pad thickness. *Mater Des* 2014; 58: 198–203.
21. American Chemistry Council. Introduction to polyurethanes: polyurethane applications, <https://polyurethane.americanchemistry.com/Applications/> (2018, accessed 18 December 2018).
22. EN 16730:2016. Railway applications – track –concrete sleepers and bearers with under sleeper pads.
23. American Railway Engineering and Maintenance-of-Way Association (AREMA). *Manual for railway engineering*. Lanham, MD: Author, 2016.
24. Branson JM, Dersch MS, Lima A de O, et al. Analysis of geometric ballast plate for laboratory testing of resilient track components. *Transp Geotech* 2019; 20.
25. Rapp CT, Edwards JR, Dersch MS, et al. Measuring concrete crosstie rail seat pressure distribution with matrix based tactile surface sensors. In: *Proceedings of the 2012 joint rail conference*, Philadelphia, PA, 17–19 April 2012.
26. Stith JC. *Railroad track pressure measurements at the rail/tie interface using Tekscan sensors*. MSc Thesis, University of Kentucky, Lexington, KY, 2005.
27. Greve MJ, Dersch MS, Edwards JR, et al. Examination of the effect of concrete crosstie rail seat deterioration on rail seat load distribution. *Transp Res Rec* 2015; 2476: 1–7.
28. McHenry MT. *Pressure measurement at the ballast-tie interface of railroad track using matrix based tactile surface sensors*. MSc Thesis, University of Kentucky, Lexington, KY, 2013.
29. Rose JG and Stith JC. Pressure measurements in railroad trackbeds at the rail/tie interface using Tekscan sensors. In: *Proceedings of the American railway engineering and maintenance of way association conference*, Nashville, TN, 19–22 September 2004.
30. McHenry MT, Brown M, LoPresti J, et al. The use of matrix based tactile surface sensors to assess the fine scale ballast-tie interface pressure distribution in railroad track. *Transp Res Rec* 2015; 2476: 23–31.
31. Greve MJ, Dersch MS, Edwards JR, et al. The effect of particle intrusion on rail seat load distributions on heavy haul freight railroads. In: *Proceedings of the 2015 international heavy haul conference*, Perth, AT, 21–24 June 2015.

32. Abadi T, Le Pen L, Zervos A, et al. Measuring the area and number of ballast particle contacts at sleeper/ballast and ballast/subgrade interfaces. *Int J Rail Technol* 2015; 4: 45–72.
33. Wnek MA. *Investigation of aggregate properties influencing railroad ballast performance*. MSc Thesis, University of Illinois at Urbana-Champaign, Urbana, IL, 2013.
34. Wang B, Martin U and Rapp S. Discrete element modeling of the single-particle crushing test for ballast stones. *Comput Geotechnic* 2017; 88: 61–73.
35. El Shahawi M and Batchelor B dV. Fatigue of partially prestressed concrete. *J Struct Eng* 1986; 112: 524–537.
36. American Concrete Institute Committee 215. *Considerations for design of concrete structures subjected to fatigue loading*. Detroit, MI: Author, 1992.